Effects of thermal treatments on the lattice properties and electronic structure of ZrH_x

R. C. Bowman, Jr.* and B. D. Craft
Mound Facility, Monsanto Research Corporation, Miamisburg, Ohio 45342

J. S. Cantrell
Chemistry Department, Miami University, Oxford, Ohio 45056

E. L. Venturini
Sandia National Laboratories, Albuquerque, New Mexico 87185
(Received 14 December 1984)

In order to examine possible sources of the discrepancies between the proton NMR parameters for ZrH_x as reported by R. C. Bowman, Jr., *et al.* [Phys. Rev. B **27**, 1474 (1983)] and C. Korn [Phys. Rev. B **28**, 95 (1983)], proton spin-lattice relaxation times (T_1), lattice parameters, and magnetic susceptibilities (χ) have been measured for high-purity ZrH_x samples in the composition range $1.5 \leq x \leq 1.9$ that had been typically annealed at 525 °C for 21 d. When these results are compared with the corresponding parameters obtained on the as-prepared ZrH_x samples of Bowman *et al.* it was found that the anneals generally had only minor effects on the proton T_1 values, lattice parameters, or $\chi(T)$ behavior. The most notable exception is a $ZrH_{1.70}$ sample that was initially composed of a mixture of δ(fcc) and ϵ(fct) phases and converted to just the ϵ phase upon annealing. Although the anneals gave small systematic decreases in the unit-cell volumes, the tetragonal distortions (i.e., c/a ratios) were not affected within experimental accuracy. Furthermore, both the proton $(T_1T)^{-1/2}$ peak and T_1T temperature dependences were also not significantly changed by these anneals. Although the $\chi(T)$ values in the ϵ phase decrease rapidly with increasing hydrogen content, a local $\chi(T)$ maximum that reflects the Pauli component from a peak in the Fermi-level density of states is observed near $x = 1.80$. The dominant $\chi(T)$ decrease is primarily attributed to reductions in the orbital contribution with the increasing tetragonal distortion. Variations in the concentrations and distributions of oxygen and paramagnetic impurities are believed to be responsible for most of the differences found in the previous studies.

I. INTRODUCTION

The role of electronic structure on the cubic-tetragonal phase transitions of the nominal-dihydride phase formed by the group-IVb metals Ti, Zr, and Hf has received considerable theoretical[1,2] and experimental[3–9] attention in recent years. In particular, the tetragonal distortion has been attributed to a solid-state analog of the classical Jahn-Teller effect[10] that involves a splitting of the transition-metal d-electron states in the region of the Fermi energy E_F. Bowman *et al.*[6] (afterwards referred to as BVCAS in this paper) and Korn[7] have provided recent summaries of the experimental observations as well as related theoretical descriptions. Independent nuclear magnetic resonance (NMR) studies[6,7] of the proton spin-lattice relaxation times (T_1) and Knight shifts (σ_K) in nonstoichiometric ZrH_x yielded very similar general conclusions. First, the dominant proton-hyperfine interaction arises from a core-polarization mechanism[11] with conduction electrons localized on the Zr $4d$ states. Second, the Jahn-Teller effect produces a resolved doublet in the electronic density of states $N(E)$ near the Fermi level for the tetragonal ϵ phase of ZrH_x from the theoretically predicted[2,12] sharp $N(E)$ peak in cubic ZrH_2. This view is also consistent with electronic specific heats,[3] photoemission spectra,[4] magnetic susceptibilities,[9] and augmented plane-wave (APW) band-theoretical calculations[2] on cubic and tetragonal ZrH_2. Finally, the peak in $N(E_F)$ occurs at hydrogen composition $x \cong 1.8$ in ϵ phase.

When the data of BVCAS and Korn[7] are compared in greater detail, some discrepancies become apparent. Many of these differences are relatively minor ones that can be attributed to small variations in sample compositions, measurement techniques, calibration procedures, and data-reduction-analysis methods. However, there are two more serious inconsistencies between the results of BVACS and Korn. First, the temperature-dependent behavior of the proton $(T_1T)^{-1}$ parameters differ throughout the entire common range of sample compositions but show the greatest variation in the region of the $(T_1T)^{-1/2}$ maximum (i.e., when $x \cong 1.8$). Second, Korn concluded that no two-phase [e.g., δ(cubic) and ϵ(tetragonal) phases] region exists at the room-temperature phase boundary while the powder x-ray diffraction (XRD) patterns of BVCAS gave clear evidence for a mixed $\delta+\epsilon$ phase in $ZrH_{1.70}$. Subsequent XRD measurements by Cantrell *et al.*[8] (afterwards referred to as CBS) confirmed the two-phase character in this $ZrH_{1.70}$ sample. The greatest differences between the ZrH_x samples of BVCAS and Korn appear to be (1) the purities of starting Zr metal

and (2) the preparation conditions of the hydride samples. BVCAS studied ZrH_x samples prepared from Marz-grade[13] Zr-metal foils where the vendor's stated purity of 99.99% (with respect to metals) has been verified by independent emission spectroscopic analysis.[14] On the other hand, Korn used Zr sponge of unspecified purity. Furthermore, Korn reported rather large paramagnetic impurity contributions to the proton T_1 relaxation times that necessitated a special analysis to extract the conduction-electron T_1 components. Phua *et al.*[15] in a series of papers have emphasized that conventional approaches to deduce diffusion and conduction-electron contributions from proton T_1 data even with rather small concentrations of paramagnetic impurities are often unreliable. Because of the high purity of their initial Zr metal (e.g., 20 ppm Fe) and absence of any anomalous effects in the rigid-lattice proton line shapes,[14] BVCAS had neglected paramagnetic impurities effects during the analysis of their proton T_1 data. The NMR and XRD samples of BVCAS had been prepared[14] by heating cleaned Zr foils to 500—600 °C with stoichiometric amounts of hydrogen gas for several hours. After equilibrium conditions had been established (i.e., pressure changes with temperature), the reactor was slowly cooled (usually overnight) to room temperature. Korn prepared his samples by heating weighed mixtures of Zr metal and ZrH_2 powders in evacuated Pyrex tubes for about 20 d at 525 °C. Korn has also suggested that annealing may affect the behavior of the tetragonal distortion as well as the NMR parameters.

The present paper reports the NMR and XRD results obtained when portions of most of the ZrH_x samples (i.e., for compositions in the range $1.5 \leq x \leq 1.9$) from the BVCAS and CBS studies were annealed at 525 °C for extended periods (usually 21 d). Furthermore, the effects of these thermal anneals on the magnetic susceptibilities were examined. With the exception of one $ZrH_{1.70}$ sample, the anneals did not alter the ZrH_x phase compositions or unit-cell parameters nor significantly modify either the composition or temperature-dependent behavior of the proton T_1 values. While one $ZrH_{1.70}$ sample changed from mixed $\delta+\epsilon$ phases to pure ϵ phase, a second $ZrH_{1.70}$ sample retained a mixture of δ and ϵ phases after the 525 °C anneal. Although differences in oxygen-impurity contents may influence the width of the two-phase region,[8] a definitive assessment could not be deduced from the current NMR and XRD experiments. In any case, the anneals did not remove most of the discrepancies with Korn results, which are now thought to be mainly due to various complications[15] from paramagnetic impurity effects on Korn's proton T_1 data as as well as possible uncertainties in his XRD data. Nevertheless, the basic soundness of the proposed Jahn-Teller mechanisms[6–8] for tetragonal distortion in ϵ-ZrH_x to produce a peak in $N(E_F)$ when $x \cong 1.8$ remains intact.

II. EXPERIMENTAL PROCEDURE

The original synthesis conditions for ZrH_x samples has been previously described.[6,8,14] Since their preparation, the ZrH_x materials had been stored in evacuated and flame-sealed glass tubes as either the initial foil pieces or powders that had been ground in a purified-argon-atmosphere glovebox. Various ZrH_x sample tubes that contained either the foils or powders with compositions in the range $1.50 \leq x \leq 1.95$ were annealed at 525 °C for 21 d with the exceptions of two tubes of $ZrH_{1.70}$ (sample No. B10) that were separately annealed for 8 and 14 d at 525 °C. After each annealing was completed, the sealed sample tube was either furnace cooled or air quenched to room temperature. No differences due to cooling technique were subsequently noted except for the air-quenched $ZrH_{1.95}$ sample that appeared to have suffered some loss in the stoichiometry to give NMR and XRD results similar to the $ZrH_{1.90}$ samples. The annealed tubes were opened in a glovebox filled with purified argon; all foil samples were ground to -200 mesh powder; and the powders divided into samples for the NMR, XRD, and magnetic-susceptibility experiments. A Cenco oven equipped with a thermocouple display and recorder that monitored the entire annealing cycle was used for these anneals. The furnace temperature did not vary by more than ± 1 °C from its nominal value.

The proton T_1 data were obtained with the normal-inversion recovery method in an identical way to the method of BVCAS. The ZrH_x samples had been sealed in evacuated 7-mm-o.d. glass tubes. The proton-resonance frequency was 34.5 MHz and measurements were performed over the temperature range between 115 and 300 K.

Two different x-ray diffractometers[8] were used to determine the XRD patterns of the annealed ZrH_x powders: a Phillips-Norelco (XRG-3000) with a theta-compensating slit and a Rigaku D/MAX automated diffractometer with a rotating-anode generator. Both XRD systems were operated in the θ-2θ scan mode using Cu $K\alpha$ radiation and a nickel filter. The Phillips generator was operated at 35 kV and 15 ma, and the Rigaku unit was operated at 50 kV and 80 ma. The XRD samples were mounted on microscope slides with double sticky transparent tape and were open to the air.[8] National Bureau of Standards silicon (sample No. 640a) was used as an internal standard. The ZrH_x samples were run in duplicate at room temperature and the unit-cell parameters were derived from the XRD patterns with full-matrix least-squares-fitting programs. All the 2θ data were reproducible to 0.05°.

The magnetic susceptibilities were derived from least-squares fits to the magnetic field dependences of the magnetizations measured between 5 and 20 kG with a S.H.E. Corporation superconducting quantum interference device magnetometer. The magnetization data were also corrected for the contributions of the Kel-F sample container. The susceptibilities were determined for temperatures between 7 and 300 K.

III. RESULTS AND DISCUSSION

A. XRD studies

The room temperature lattice parameters a and c for the unannealed (i.e., as originally prepared for the BVCAS and CBS studies) ZrH_x materials and those samples annealed at 525 °C are summarized in Table I and are com-

TABLE I. Summary of unit-cell parameters at 293 K for ZrH_x samples from x-ray diffraction measurements.

x	Sample number	Phase	Anneal conditions	a (nm)	c (nm)	c/a	V (nm)^3
1.997	B1	ϵ	U[a]	0.498 25(9)	0.444 88(9)	0.8929(8)	0.110 44(9)
1.950	B9	ϵ	U	0.497 84(9)	0.445 08(9)	0.8940(8)	0.110 31(9)
1.901	B4	ϵ	U	0.497 29(8)	0.445 41(9)	0.8957(8)	0.110 15(9)
1.901	B4	ϵ	525 °C, 21 d	0.496 89(6)	0.444 97(5)	0.8955(6)	0.109 86(6)
1.852	B8	ϵ	U	0.496 24(9)	0.446 70(8)	0.9002(8)	0.110 00(9)
1.852	B8	ϵ	525 °C, 21 d	0.495 47(5)	0.446 71(6)	0.9016(6)	0.109 66(6)
1.835	B7	ϵ	U	0.495 72(6)	0.447 50(5)	0.9027(6)	0.109 97(6)
1.835	B7	ϵ	525 °C, 21 d	0.495 90(4)	0.446 10(5)	0.8996(5)	0.109 70(5)
1.801	B3	ϵ	U	0.493 77(8)	0.450 56(10)	0.9125(9)	0.109 85(9)
1.801	B3	ϵ	525 °C, 21 d	0.494 37(4)	0.450 18(4)	0.9106(4)	0.109 55(4)
1.776	B12	ϵ	U	0.493 00(9)	0.452 04(9)	0.9169(8)	0.109 87(9)
1.776	B12	ϵ	525 °C, 21 d	0.492 18(3)	0.451 91(4)	0.9182(3)	0.109 47(6)
1.750	B5	ϵ	U	0.491 67(8)	0.454 18(8)	0.9237(7)	0.109 79(9)
1.750	B5	ϵ	525 °C, 21 d	0.491 22(4)	0.453 17(4)	0.9225(4)	0.109 35(6)
1.701	B15	ϵ	U	0.489 90(9)	0.457 28(10)	0.9334(8)	0.109 75(9)
1.701	B15	δ	U	0.478 58(9)			0.109 61(9)
1.701	B15	ϵ	525 °C, 21 d	0.489 15(8)	0.456 69(9)	0.9336(8)	0.109 27(9)
1.701	B15	δ	525 °C, 21 d	0.477 83(11)			0.109 10(10)
1.701	B10	ϵ	U	0.490 53(8)	0.457 05(8)	0.9321(8)	0.109 89(9)
1.701	B10	δ	U	0.478 41(8)			0.109 50(9)
1.701	B10	ϵ	525 °C, 8 d	0.489 68(11)	0.457 29(10)	0.9338(9)	0.109 65(10)
1.701	B10	δ	525 °C, 8 d	0.478 59(12)			0.109 62(11)
1.701	B10	ϵ[b]	525 °C, 14 d	0.489 38(12)	0.456 72(11)	0.9333(9)	0.109 38(11)
1.651	B13	δ	U	0.478 52(12)			0.109 57(11)
1.651	B13	δ	525 °C, 21 d	0.477 70(5)			0.109 01(5)
1.603	B2	δ	U	0.478 50(9)			0.109 56(8)
1.603	B2	δ	525 °C, 21 d	0.477 75(5)			0.109 04(5)
1.551	B11	δ	U	0.478 43(11)			0.109 51(9)
1.551	B11	δ	525 °C, 21 d	0.477 54(5)			0.108 90(6)
1.501	B6	δ	U	0.478 57(10)			0.109 56(9)
1.501	B6	δ	525 °C, 21 d	0.477 59(5)			0.108 94(6)

[a] U represents unannealed (as-prepared).
[b] Annealed to pure ϵ phase.

pared in Fig. 1. The tetragonal distortion of the ϵ-phase unit cells are clearly shown in Figs. 1 and 2. The lattice parameters for the unannealed ZrH_x samples given in Table I are slightly different from the 293 K values reported by CBS. Both sets of parameters had been obtained from the same experimental XRD diffraction patterns. However, during the present comprehensive analysis of the XRD patterns of the annealed ZrH_x samples it was found that as the c/a ratios changed rapidly for stoichiometries between $x=1.75$ and 1.90 some of the diffraction lines actually crossed in their 2θ values, which is shown in Table II. Those lines which cross in 2θ values as x changes include: [113] and [222] at $x=1.801$, [004] and [420] at $x=1.901$, [313] and [402] at $x=1.776$, and [004] and [331] at $x=1.776$. A detailed discussion of this behavior, which will also identify some other lines that cross in 2θ values, will be presented in a future publication in a more specialized crystallography journal. Since the tetragonal distortion can change the relative 2θ values of the diffraction lines, considerable care must be exercised during the indexing of the XRD patterns when the diffraction lines can cross as shown in Table II. Consequently, a very careful evaluation of the XRD data for the unannealed as well as annealed ZrH_x samples produced reassignments of some of the Miller indices originally chosen by CBS. This analysis reduced the errors of the calculated unit-cell parameters and also decreased some of the "scatter" in composition dependences of these quantities. All of the ZrH_x samples were subjected to thorough numerical data-fitting analysis that included full-matrix least-squares fits to all the available XRD data. Therefore, the lattice parameters given in Table I are believed to be the most reliable values that can be obtained for these ZrH_x samples.

Figures 1 and 2 directly compare the effects of the 525 °C anneals on the ZrH_x unit-cell constants at room temperature (293 K) and the corresponding c/a ratios, respectively. Within the experimental precision of the XRD data these anneals show little influence on a, c, or the c/a ratio. Furthermore, the c/a ratios for both unannealed and annealed ZrH_x samples are shown in Fig. 2 to be in good agreement with the ratios measured by Korn,[7] Korst,[16] and Barraclough and Beevers.[17] However, the expanded scale plot of the unit-cell volumes (V) in Fig. 3 does reveal small systematic volume decreases upon annealing for all the ZrH_x compositions studied. Figure 3

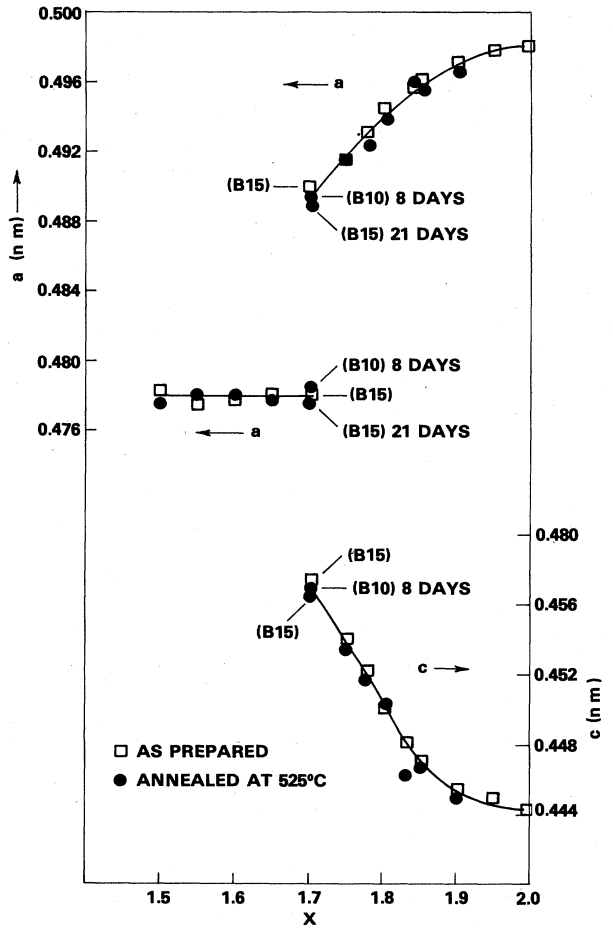

FIG. 1. Stoichiometry dependences of room temperature (293 K) unit-cell axes a and c for unannealed (□) and 525 °C annealed (●) ZrH_x samples. Error bars not included fall within the symbols.

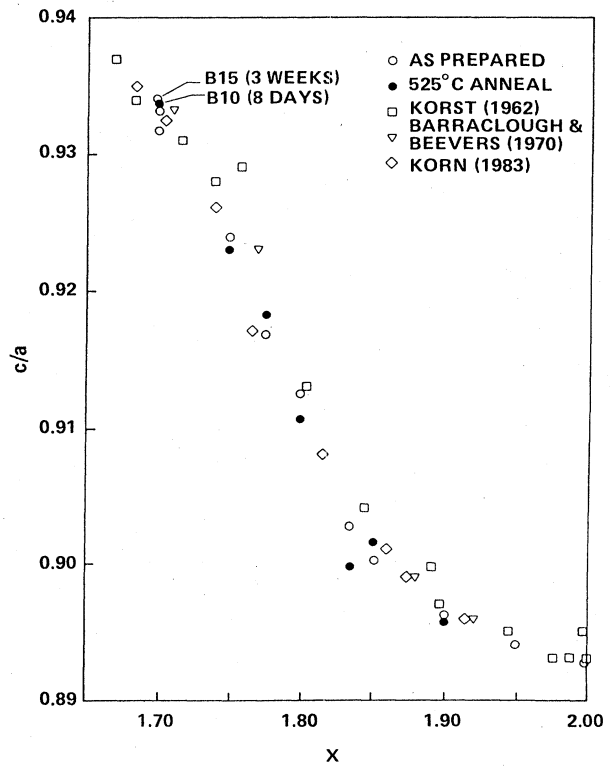

FIG. 2. Stoichiometry dependences of c/a ratios for unannealed (○) and 525 °C annealed (●) ZrH_x samples. The errors based upon root-mean-square standard deviations fall within the symbols.

also presents the ZrH_x volumes reported by Korn.[7] The fractional changes in volume ($\Delta V/V_u$) are the differences (ΔV) between the unit-cell volumes for the unannealed and annealed samples divided by the unannealed volume (V_u). The stoichiometry dependence of $\Delta V/V_u$ is given in Fig. 4 where a linear decrease is observed as the hydrogen content increases. Since the hydrogen dissociation pressures increase[18] as x approaches 2.0, loss of hydrogen gas from the ZrH_x samples during the anneals cannot be responsible because the largest volume decreases occur for anneals of samples with the smallest composition (i.e., the ones with the lowest dissociation pressure). If hydrogen loss was the cause, the $\Delta V/V_u$ behavior would show a completely opposite change to that seen in Fig. 4.

The decrease in volume upon annealing could be the result of a redistribution of the hydrogen atoms to more uniformly occupy the tetrahedral sites such that any hydrogen-hydrogen repulsions are minimized. This decrease in H-H repulsion may reduce residual stresses in the lattice to produce a corresponding decrease in the unit-cell volumes. Removal of dislocations or intrinsic

TABLE II. Comparisons of selected x-ray (Cu K_α) 2θ values (in degrees) for selected [hkl] Miller indices of several ϵ-phase ZrH_x samples. The asterisks (*) denote equal 2θ or crossover 2θ for two diffraction lines with [hkl] values in adjacent columns.

x	[222]	[113]	[331]	[420]	[004]	[402]	[313]
1.997	67.87	68.67	85.52	87.57	87.76	90.36	91.10
1.950	67.89	68.64	85.59	87.66*	87.71	90.42	91.12
1.901	67.92	68.61	85.70	87.78*	87.62	90.49	91.13
1.852	67.94	68.44	85.89	88.01	87.31	90.60	91.07
1.835	67.93	68.34	85.98	87.11	88.13	90.65	91.02
1.801	67.92*	67.94	86.33	88.57	86.37	90.81*	90.82
1.776	67.91	67.75	86.47*	88.74	86.02*	90.86	90.72
1.750	67.90	67.47	86.71	89.04	85.52	90.98	90.59
1.701	67.89	67.08	87.03	89.45	84.80	91.13	90.39

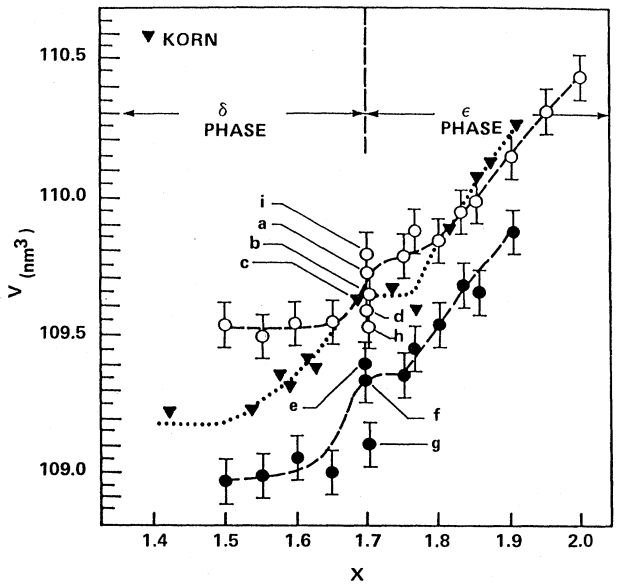

a - ϵ (B15) UNANNEALED
b - δ (B10) ANNEALED 8 DAYS
c - ϵ (B10) ANNEALED 8 DAYS
d - δ (B15) UNANNEALED
e - ϵ (B10) ANNEALED 14 DAYS
f - ϵ (B15) ANNEALED 21 DA
g - δ (B15) ANNEALED 21 DA
h - δ (B10) UNANNEALED
i - ϵ (B10) UNANNEALED

FIG. 3. Stoichiometry dependences of room temperature (293 K) unit-cell volumes V for unannealed (○) and 525 °C annealed (●) ZrH_x samples. Volumes reported by Korn (Ref. 7) are plotted with symbols ▼. Indicated error bars are based upon root-mean-square values.

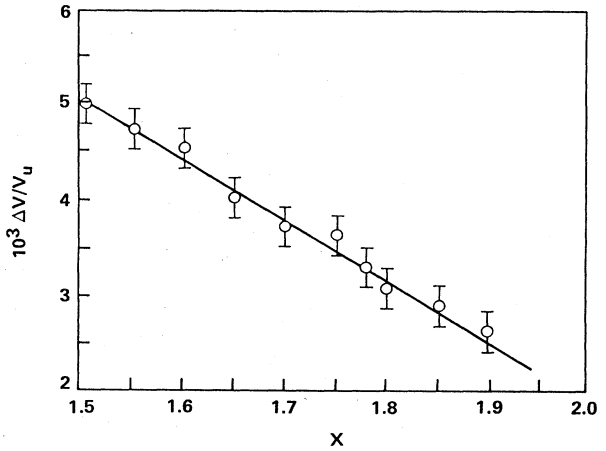

FIG. 4. Fractional change in ZrH_x unit-cell volumes ($\Delta V/V_u$) between unannealed and 525 °C anneals. Quantities calculated from volumes in Table I and indicated error bars are based upon root-mean-square values.

point defects (e.g., Zr-metal vacancies) during the anneal could also produce a small volume decrease.[7] Small decreases in the line widths of higher-angle XRD peaks were observed upon annealing, which is consistent with removal of strain or increased sample homogeneity. However, the present experimental conditions do not permit quantitative evaluation of this behavior. Furthermore, it is difficult to explain the systematic decrease in $\Delta V/V_u$ with x for the stress-release mechanism since the microhardness of the ZrH_x phases[17] greatly decrease with x, which should facilitate defect annihilations at the larger compositions. Hence, $\Delta V/V_u$ would become larger as x increased, which is again opposite to the behavior in Fig. 4.

The solution of oxygen into the ZrH_x lattice provides an alternative mechanism for the volume shrinkage found after the 525 °C anneals. Although various efforts have been made to minimize oxygen contamination in these ZrH_x samples (i.e., surface cleaning, sample handling in gloveboxes with high-purity-argon atmospheres, storage in evacuated sealed tubes, etc.), oxygen—particularly on surfaces—cannot be avoided. In fact, ion-sputtered cleaned surfaces of Zr metal and hydrides have been observed[19] to rapidly form ZrO_2 films with thicknesses of several nm from the residual oxygen in a 10^{-9} Torr vacuum. With photoelectron spectroscopy Berezina *et al.*[20] found that oxygen from a ZrO_2 surface layer will rapidly diffuse in the bulk Zr metal at temperatures above 450 °C. Consequently, surface oxygen on the ZrH_x samples could diffuse into the bulk when annealed at 525 °C for many days. Although hydrogen occupies the tetrahedral interstitial sites in ZrH_x,[14] the larger octahedral sites are vacant. Since oxygen is octahedrally coordinated in the binary oxides[21] Zr_3O, ZrO, and ZrO_2 as well as in various ternary Zr-based oxides,[22–24] a finite solubility of oxygen in octahedral sites seem possible to give a ternary ZrO_yH_x phase.[25] The formation of chemical bonds between the octahedral oxygen and surrounding Zr atoms could decrease their initial separations to give a reduced unit-cell volume. Nevitt *et al.*[22] found the cubic lattice parameter a for the ternary Zr-Ir-O, Zr-Pt-O, and Zr-Rh-O alloys with the $Fd3m$ structure to decrease slightly with increases in oxygen content. Furthermore, when the stoichiometry of fcc LaH_x increases above 2.0, the additional hydrogen occupies the octahedral sites and the lattice constant and volume significantly decrease.[26] Hence, the solution of surface oxygen during the extended 525 °C anneals of ZrH_x could produce the small volume decrease shown in Fig. 3. With oxygen in the octahedral sites, repulsive interactions with the hydrogen atoms in neighboring tetrahedra appear likely in the context of a simple hard-sphere model. This effect would favor the trapping of hydrogen tetrahedral vacancies near the oxygen atoms. As x increases, there are fewer vacancies and the number of hydrogen atoms surrounding the oxygen becomes larger. Consequently, any oxygen-induced reduction of the ZrH_x unit-cell volume would become less effective when the stoichiometry increases towards 2.0 and all octahedral sites are completely coordinated by eight hydrogen atoms. Thus, the $\Delta V/V_u$ decrease shown in Fig. 4 would result.

The suggestion by Korn[7] that annealing influences the ZrH_x unit-cell parameters through the removal of order-disturbing centers such as dislocations would be an additive contribution to the oxygen effects proposed in the preceding paragraph. The randomization of hydrogen atoms to minimize hydrogen-hydrogen repulsions is another possible effect of anneals. Unfortunately, the

available XRD data cannot definitely establish whether one mechanism is dominant although the oxygen effect is tentatively favored. In principle, all these effects could combine to produce the small decreases in unit-cell volumes for the annealed ZrH_x samples, which are greatest for the lower x values (i.e., $1.50 \leq x \leq 1.65$) as shown in Figs. 3 and 4.

Holmberg and Dagerhamn[21] reported the formation of $ZrO_{0.33}$ (i.e., Zr_3O) as oxygen diffuses into Zr-metal lattice during 600 °C anneals. They also reported that oxygen randomly occupies octahedral interstices and that after an initial volume increase as oxygen dissolves in the metal, there is a slight decrease in the unit-cell volume. The crystallographic properties of the Zr_3O phase are well characterized.[21] The Zr_3O phase has been tentatively identified in the present XRD patterns for the ZrH_x samples with $x=1.501$, 1.551, 1.603, and 1.651 where the stronger XRD peaks (e.g., $[111]_{100}$ and $[002]_{50}$ at the 2θ values 36.26° and 34.46°, respectively) of the Zr_3O phase are well resolved and seen considerably above background. The amounts of Zr_3O in these ZrH_x samples are estimated to be on the order of 1 at. % or less. The amount of the Zr_3O detected in the annealed ZrH_x samples ranges from about 1.0 at. % for $x=1.501$ to less than 0.5 at. % for $x=1.651$. This Zr_3O phase is barely detectable in the unannealed ZrH_x samples. Consequently, an effect of annealing these ZrH_x samples appears to be the diffusion of surface oxygen into the bulk lattice. However, there are problems with making an unambiguous identification of Zr_3O as a minor contaminant of ZrH_x. Although the strongest diffraction lines for Zr_3O correspond to well-resolved peaks in the ZrH_x XRD data, these weak lines are also in reasonable agreement with the strongest XRD lines of the hexagonal α phases of ZrH_x (i.e., the $[002]_{30}$ and $[101]_{100}$ peaks at the 2θ values 34.84° and 36.51°, respectively, which are somewhat dependent on hydrogen content). Furthermore, oxygen contents at approximately 1 at. % have been reported[27] to stabilize the α phase in ZrH_x in the ZrO_yH_x phase diagram (see Fig. 7b in Ref. 27). In support of the present studies, neutron-activation and vacuum-fusion analyses were performed on several ZrH_x samples and yielded oxygen contents in the range 1 000—4 000 wppm, which establishes an upper limit of about 1 at. % oxygen. However, the measured oxygen contents could not be correlated with either hydride stoichiometry or thermal treatment. Furthermore, these methods cannot distinguish between the different chemical forms of oxygen—namely, ZrO_2 on the surface,[19,20] precipitation as a binary oxide (i.e., Zr_3O or ZrO), or oxygen in a ternary ZrO_yH_x phase. Thus, the weak "impurity" XRD peaks primarily seen in the annealed δ-phase ZrH_x samples can be alternatively interpreted as precipitated Zr_3O or the stabilization of some α-ZrH_x phase. At hydrogen contents above $x=1.70$, the [200] diffraction line of the ϵ phase with a 2θ value of 36.26° obscures the peaks at this 2θ value for both the Zr_3O and α-ZrH_x phases. Thus, the XRD patterns cannot detect the presence of these species in ZrH_x samples with $x \geq 1.70$.

In contrast to several previous XRD studies[6,8,16,18] that indicated a limited mixed-phase region between the δ and ϵ phases at room-temperature conditions, Korn[7] reported that the δ-ϵ phase boundary at $x=1.65$ has a discontinuous transition without a mixed-phase region. The two unannealed $ZrH_{1.70}$ samples (i.e., B10 and B15) are shown in Fig. 1 and Table I to contain both the δ and ϵ phases. Upon annealing, one sample (B15) remains two phase with virtually no change in the phase ratio as inferred from the XRD intensities while the second sample (B10) completely converts (within the accuracy of the XRD method) into the ϵ phase. The phase diagram of Ells and McQuillan[27] for the ternary ZrO_yH_x system indicates that at 750° the presence of about 1 at. % oxygen can stablize the ϵ phase. When the hydrogen content is less than 60 at. %, more than 1 at. % of oxygen is required[27] to stabilize the ϵ phase (i.e., 2.5 at. % oxygen is needed for a 59 at. % hydrogen sample) at 750 °C. Thus, an extended 525 °C anneal of a mixed (i.e., δ and ϵ phase) $ZrH_{1.70}$ sample could transform to pure ϵ phase if sufficient oxygen is available. Since the B10 $ZrH_{1.70}$ sample did convert to the ϵ phase while the B15 sample remains two phase following a 21-d anneal at 525 °C, the oxygen content is presumably lower in the B15 material. However, the oxygen-elemental analyses on these samples were not sufficiently reliable to identify any differences in oxygen contents between the B10 and B15 sample either before or after the anneals. Korn[7] had used Zr sponge of unspecified purity to prepare his ZrH_x samples. This type of Zr is normally difficult to clean and probably contained significant quantities of surface oxide, which can diffuse into the bulk lattice and can stablize the ϵ phase throughout the entire ZrH_x stoichiometry range that would be two phase in a high-purity system. Although no isothermal section is available for the ternary ZrO_yH_x phase diagram at 525 °C, it is probably very similar to the 750 °C diagram in Fig. 7b of Ref. 27. The most likely explanation for the XRD data of Korn not showing a two-phase region near $x \cong 1.70$ is the presence of enough oxygen to completely stabilize the ϵ phase for compositions down to about $x=1.65$ where only the δ phase exists at all temperatures.

B. Proton NMR studies

BVCAS (Ref. 6) has provided a detailed description of the relationships between proton NMR parameters and the electronic structure properties of transition-metal hydrides where particular emphasis was focused upon the ZrH_x system. Consequently, only those key features that are necessary for the present situation will be briefly summarized. The hyperfine interaction[11] with unpaired conduction electrons is presumed to be the dominant proton T_1 relaxation mechanism for the present high-purity ZrH_x samples since the covered temperature range (i.e., $T \leq 300$ K) is too low for any effect from the diffusion terms[28] and possible paramagnetic relaxation contributions[15] should also be small. Korn[7] reported significant paramagnetic effects in his T_1 data, and his samples appear to be much less pure than the present samples where the starting Zr foil contained[6] only about 20 ppm Fe.

Within the free-electron approximation[11] the conduction-electron contribution to the proton spin-lattice relaxation time (T_{1e}) for transition-metal hydrides is given by the expression[6,8]

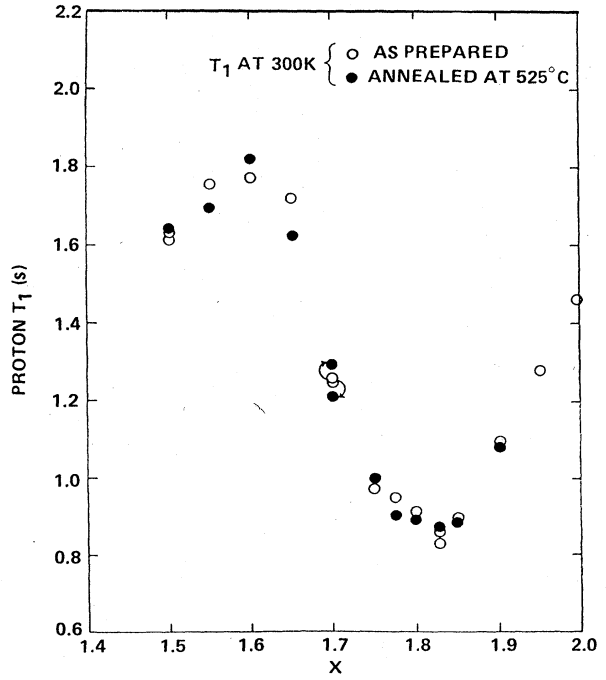

FIG. 5. Comparison of proton T_1 data at 300 K for unannealed and annealed ZrH_x samples.

$$R(T)=(T_{1e}T)^{-1}$$
$$=C_H\{[H_{\rm hf}(s)N_s(E_F)]^2+[H_{\rm hf}(d)N_d(E_F)]^2q\}\ , \quad (1)$$

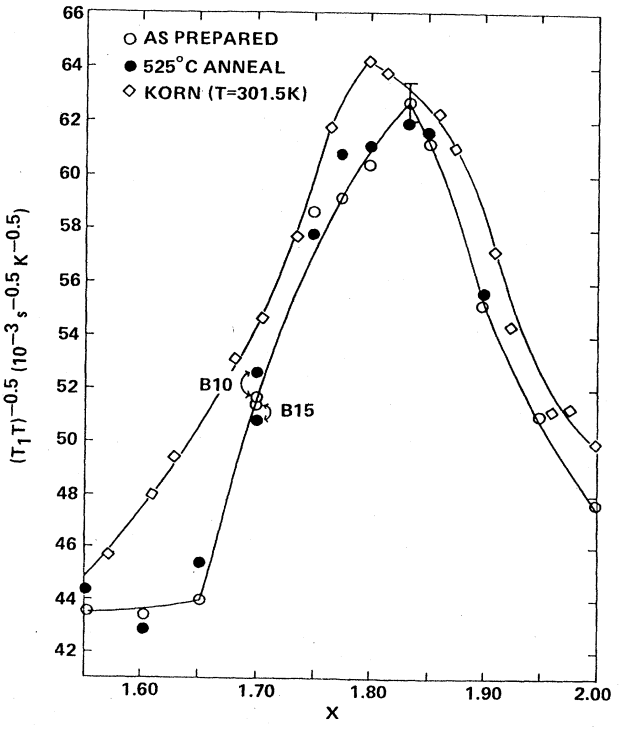

FIG. 6. Composition dependence of proton $(T_1T)^{-1/2}$ parameters at 300 K for unannealed and annealed ZrH_x samples. The similar parameters of Korn (Ref. 7) are also presented.

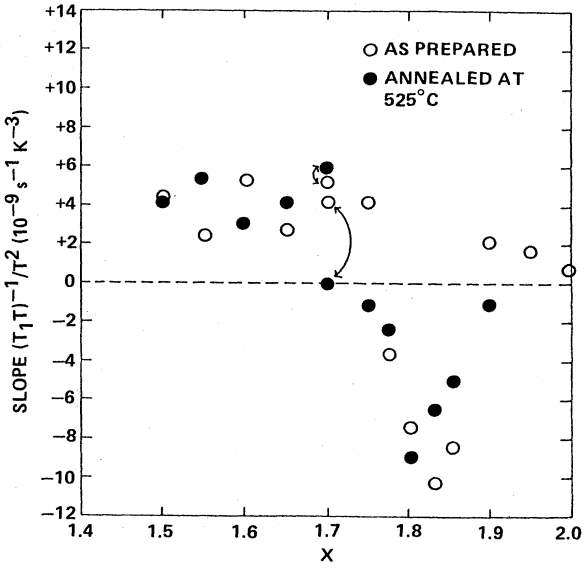

FIG. 7. Composition dependence of proton T_1 temperature coefficients for unannealed and annealed ZrH_x samples.

where C_H is a constant;[8] $N_s(E_F)$ and $N_d(E_F)$ are the s- and d-band density of states at the Fermi level, respectively; $H_{\rm hf}(s)$ is the Fermi-contact hyperfine field for unpaired s electrons at E_F; $H_{\rm hf}(d)$ is the core-polarization hyperfine field of the spin-paired proton s orbitals below E_F from the unpaired metal d electrons at E_F as described by Narath.[11] The negative proton Knight shifts[6] for ZrH_x as well as APW band-theory calcula-

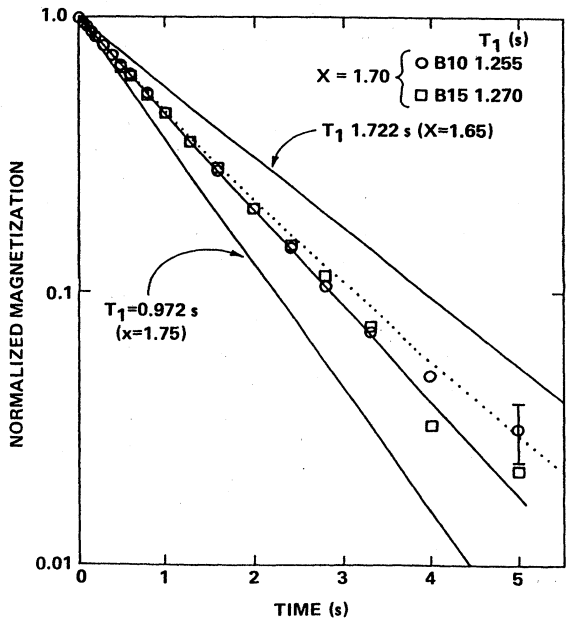

FIG. 8. Proton spin magnetization recoveries at 300 K for unannealed ZrH_x samples. Solid lines are least-squares exponential fits to data for $ZrH_{1.65}$, $ZrH_{1.70}$(B15), and $ZrH_{1.75}$. The dotted line is obtained with expression $0.5[\exp(-t/1.722)+\exp(-t/0.972)]$. See text for discussion.

tions[2,12] for ZrH_2 indicate $N_d(E_F) \gg N_s(E_F)$; hence, the second term dominates Eq. (1). Thermal broadening of the electron distribution with increasing temperature can produce a temperature dependence in $R(T)$ through the relation

$$R(T)=R(0)\left[1+\frac{\pi^2 k_B^2 T^2}{3}\frac{1}{N(E)}\frac{d^2N(E)}{dE^2}\bigg|_{E=E_F}\right], \quad (2)$$

where k_B is the Boltzmann's constant. As long as $N(E_F)$ is not strongly dependent upon extraneous factors, the major influence to the $R(T)$ temperature dependence will be the relative position of E_F to any local sharp structures (e.g., peaks) in the density of states.[6,8]

The proton T_1 relaxation times for the 525 °C-annealed ZrH_x samples have been measured under essentially identical conditions as were used for the original samples of BVCAS. The comparison of the two sets of 300 K T_1 data given in Fig. 5 reveals only minor differences where a pronounced minimum occurs for a stoichiometry just above $x=1.8$. Furthermore, Fig. 6 shows that the 300 K $(T_1T)^{-1/2}$ parameters, which according to Eq. (1) are directly proportional to $N(E_F)$, are also not significantly altered by the 525 °C anneals. Within the precision of the data, the $(T_1T)^{-1/2}$ peak for the annealed samples has not shifted from the position at $x=1.83$ in the initial BVCAS measurements. Figure 6 also includes the 301.5 K $(T_1T)^{-1/2}$ values reported by Korn[7] which are seen to be slightly (but systematically) larger than the present and BVCAS results. Korn's data place the $(T_1T)^{-1/2}$ peak at $x=1.80$. The temperature dependences from least-squares fits of $(T_1T)^{-1}$ versus T^2 plots for all the unannealed and annealed high-purity ZrH_x samples are compared in Fig. 7. As observed previously by BVCAS, the temperature dependence becomes strongly negative only when $x=1.8$. Furthermore, Fig. 7 shows that the 525 °C anneals had virtually no effect on this behavior.

BVCAS attributed the negative temperature coefficients of $R(T)$ and $\sigma_K(T)$ for stoichiometries near $x=1.8$ to the Fermi-level position at the top of the densities-of-states peak produced by the Jahn-Teller effect. However, Korn[7] reported only positive temperature dependences for $R(T)$-versus-T^2 plots where the smallest slope occurs near $x=1.8$. Korn has mistakenly assumed that at a local maximum the second derivative of a function [i.e., $d^2N(E)/dE^2$ in Eq. (2)] is small and increases on either side of this peak. In fact, only the first derivative vanishes at the peak while a negative second derivative actually defines the local maximum and the magnitude of this negative parameter directly reflects the sharpness of the peak. Although Korn had attempted to eliminate the paramagnetic contributions to the temperature dependences of his T_1 data, it now appears that he was only partially successful for his samples. Thus, an excessive positive temperature dependence apparently remained in all of his results to shift the expected negative temperature coefficients above zero as shown in Fig. 13(a) of Korn's paper, where the strong dip near $x=1.8$ is quite clear. Because of the higher purities of the BVCAS and present samples, the paramagnetic relaxation contributions are now much smaller and the $R(T)$ temperature dependences primarily correspond to conduction-electron

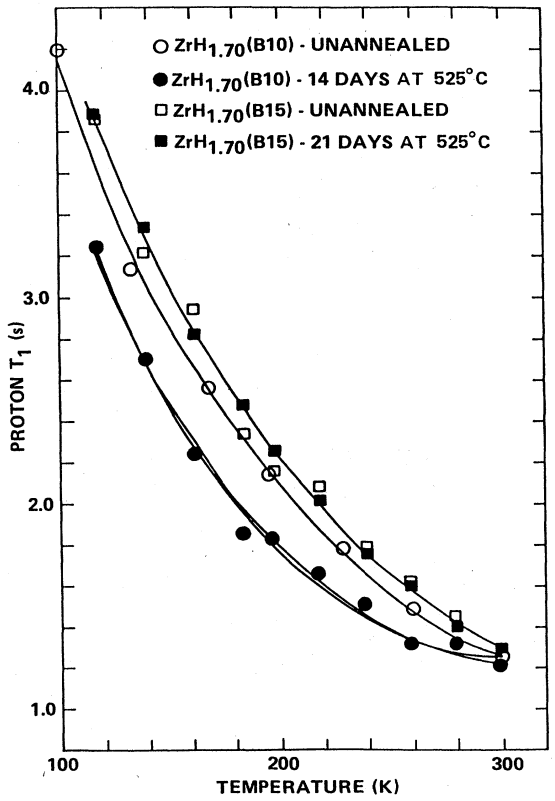

FIG. 9. Temperature dependence of proton T_1 for two $ZrH_{1.70}$ samples before and after 525 °C anneals. Curves through data points are merely visual aids.

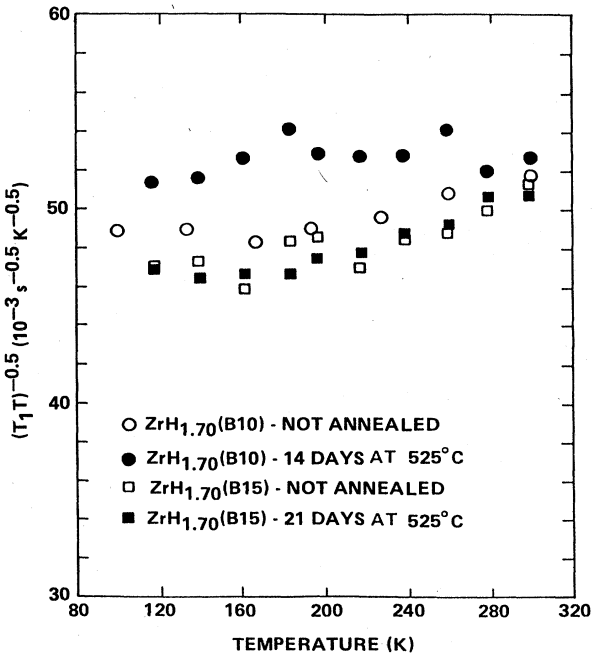

FIG. 10. Temperature dependence of proton $(T_1T)^{-1/2}$ parameters for $ZrH_{1.70}$ samples of Fig. 9 before and after 525 °C anneals.

behavior [i.e., in accord with Eq. (2) predictions] as shown in Fig. 7 where the negative peak at $x=1.8$ is essentially independent of the thermal treatment.

As described in the preceding section, x-ray diffraction indicates that the two unannealed $ZrH_{1.70}$ samples (i.e., B10 and B15) are two phase and consist of approximately equal amounts of the δ and ϵ phases. Figure 8 shows the experimental magnetization data points from the 300 K T_1 measurements for these two unannealed samples. Exponential lines can represent both sets of data points for nearly two decades of decay. This result was somewhat surprising since the T_1 values for the neighboring δ-$ZrH_{1.65}$ and ϵ-$ZrH_{1.75}$ samples differ by a factor of 2. When the dotted curve in Fig. 8 calculated for total magnetization decay from equal amounts of these latter samples are compared with the $ZrH_{1.70}$ data points, two observations are possible. First, the data points are better represented by the exponential lines than the computed two-phase curve although the data for the B10 $ZrH_{1.70}$ sample show systematic positive deviations at the longest times where accuracy is lower. Second, measured T_1 values for the two $ZrH_{1.70}$ samples in Fig. 8 are just slightly less (i.e., about 6% smaller) than the mean of the T_1 (300 K) values for the neighboring single-phase samples. These results are consistent with the previously proposed[6] mixed δ- and ϵ-phase region for $1.65(2) \leq x \leq 1.74(2)$ where $N(E_F)$ changes smoothly (if somewhat rapidly) with hydrogen content for these stoichiometries.

The temperature-dependent behavior of the proton T_1 and $(T_1T)^{-1/2}$ parameters for the unannealed and 525 °C annealed $ZrH_{1.70}$ samples are summarized in Figs. 9 and 10, respectively. Although the annealing treatments had virtually no effect on these parameters for the B15 sample, systematic T_1 decreases and $(T_1T)^{-1/2}$ increases are found for the B10 sample under similar conditions. Since the XRD measurements have shown that the B15 sample remained two phase with no significant variation in the relative δ and ϵ contents after the anneals, no change in the proton parameters is quite satisfying. However, the conversion of the B10 sample to pure ϵ phase after a 14-d anneal at 525 °C does clearly change the proton parameters. The increase in $(T_1T)^{-1/2}$ upon annealing implies that $N(E_F)$ became slightly larger in the pure ϵ phase at $x=1.70$. This behavior probably corresponds to the relative Fermi level position on the lower peak produced by the Jahn-Teller tetragonal distortion as shown in Fig. 9 of BVCAS. Unfortunately, the proton NMR parameters provide little new insight into why one sample (i.e., B10) converts into pure ϵ phase upon annealing while the second nominally identical sample (i.e., B15) remains mixed phase. The proton T_1 values for the unannealed B10 sample are slightly smaller than the values for the unannealed B15 sample and may correspond to either the small differences in hydrogen content or the presence of a slight additional paramagnetic resonance contribution in the B10 sample. However, the differences are too small to be considered significant given the $\pm 5\%$ uncertainties in the experimental relaxation times.

C. Magnetic susceptibility studies

The bulk magnetic susceptibilities of paramagnetic transition-metal hydrides have often been related[29–32] to the electronic structures of these materials. In general, $\chi(T)$ will consist of several components as follows:

$$\chi(T)=\chi_P(T)+\chi_{\rm dia}+\chi_L+\chi_{\rm orb}+\chi_{\rm mi}(T)\ , \tag{3}$$

where the diamagnetic contribution from ion cores ($\chi_{\rm dia}$), the Landau diamagnetism of the conduction electrons (χ_L), and orbital (i.e., Van Vleck) paramagnetism $\chi_{\rm orb}$ are usually temperature independent. Although $\chi_{\rm orb}$ is generally quite large in transition-metal systems,[1,33] the $\chi_{\rm dia}$ and χ_L terms normally give only small contributions to $\chi(T)$. A temperature-dependent contribution $\chi_{\rm mi}(T)$ can arise from either ferromagnetic or superparamagnetic impurities. The conduction-electron Pauli term $\chi_P(T)$ is often temperature dependent in transition metals. When the thermal broadening of the Fermi distribution in the electronic states is responsible, the Pauli term is given by[9,29,33]

$$\chi_P(T)=\chi_P(0)\left\{1+\tfrac{1}{6}\pi^2k_B^2T^2\left[\frac{1}{N(E)}\frac{d^2N(E)}{dE^2}-\left[\frac{1}{N(E)}\frac{dN(E)}{dE}\right]^2\right]_{E=E_F}\right\}, \tag{4}$$

where

$$\chi_P(0)=\mu_B^2N(E_F)/[1-JN(E_F)]\ , \tag{5}$$

μ_B is the Bohr magneton, J is the exchange-correlation integral, and $\chi_P(0)$ is the Pauli paramagnetism for noninteracting *sp* and *d* electrons. Although it is great oversimplification[1] to assume that changes in $\chi(T)$ only reflect changes in $N(E_F)$—especially since $\chi_{\rm orb}$ is substantial in most transition metals, the susceptibility is quite sensitive to the electronic structure and has closely corresponded to the hydrogen-induced modifications in $N(E_F)$ inferred from proton NMR measurements in several metal hydrides.[29,31,32]

Several groups[3,9,34,35] have previously measured the magnetic susceptibilities of ZrH_x. Most of these studies have been complicated by nonideal paramagnetic behavior that have been variously attributed to "ferromagnetic" impurities. However, the tendency of $\chi(T)$ to decrease as the hydrogen content increases from Zr metal to the dihydride was noted by all these authors. Markin and Savin[9] have recently reported a χ maximum near $x=1.9$. An examination of the purities of the ZrH_x samples used for these χ measurements[3,9,34,35] as well as anomalous proton linewidths in impure ZrH_x samples[14] lead to the supposition that Fe impurities are probably responsible for the "ferromagnetic" contributions to χ. Although Fe does

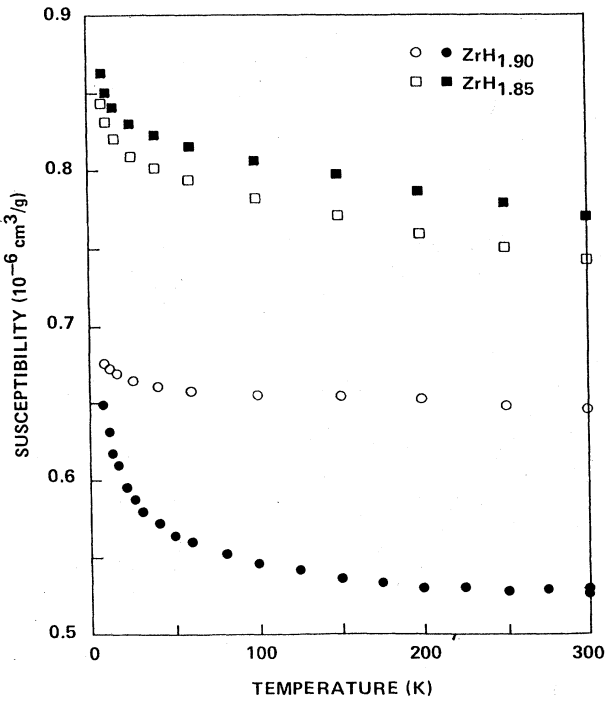

FIG. 11. Magnetic susceptibilities $\chi(T)$ for two as-prepared (open symbols) and 525 °C annealed (closed symbols) ZrH_x samples.

not carry a magnetic moment in Zr metal,[36] changes in the electronic structure upon hydriding or possible precipitation of impurity phases apparently generate extraneous magnetic effects in the ZrH_x phases. Consequently, minimal concentrations of Fe (as well as other potential magnetic impurities) are highly desirable for reliable assessments of $\chi(T)$ in ZrH_x.

As part of a general study[37] of the magnetic properties of ZrH_x with $0 \leq x \leq 2.0$, the magnetic susceptibilities have been measured for several of the as prepared and 525 °C annealed high-purity ZrH_x samples. Representative $\chi(T)$ data for some of these samples are presented in Figs. 11 and 12. The temperature dependences have been least-squares fitted with the expression

$$\chi(T)=\chi(0)[1+B_x T^2]+C_x/T\ , \tag{6}$$

where B_x and C_x are empirical constants.[38] Figure 13 compares the behavior of $\chi(300\ \text{K})$ and $\chi(0)$ as the ZrH_x stoichiometry varies between $x=1.50$ and 1.997. Although these parameters are nearly independent of hydrogen content in the δ phase ($x \leq 1.65$), both decrease rapidly (i.e., almost a factor of 3 as x approaches 2.0) with increasing stoichiometry in the ϵ phase. However, the line drawn through most of the $\chi(0)$ data reveals a local maximum at $x=1.83$. [The identical composition of the proton $(T_1T)^{-1/2}$ peak.] The dominant factor in the $\chi(T)$ decrease shown in Fig. 13 is probably a reduction in the χ_{orb} term with the increasing tetragonal distortion of the ϵ phase. This view is consistent with Switendick's qualitative theoretical analysis of $\chi(T)$ and the ZrH_x electronic structure.[2] However, a more detailed comparison of χ_{orb} with electronic structure requires explicit computations of

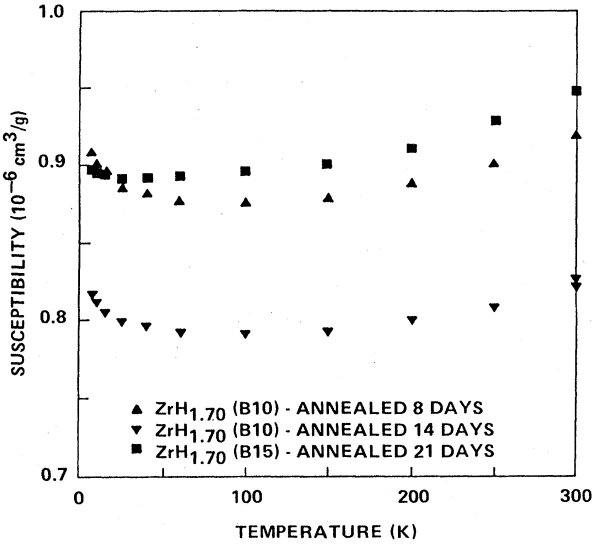

FIG. 12. Magnetic susceptibilities for three 525 °C annealed $ZrH_{1.70}$ samples.

the d-band energy levels in nonstoichiometric ϵ-phase ZrH_x, which are not currently available. The $\chi(0)$ maximum at $x=1.83$ is attributed to an increase in the Pauli term, which is superimposed on the χ_{orb} decrease, when the Fermi level moves through the $N(E)$ peak as described by BVCAS. Figure 13 also shows that $\chi(T)$ has

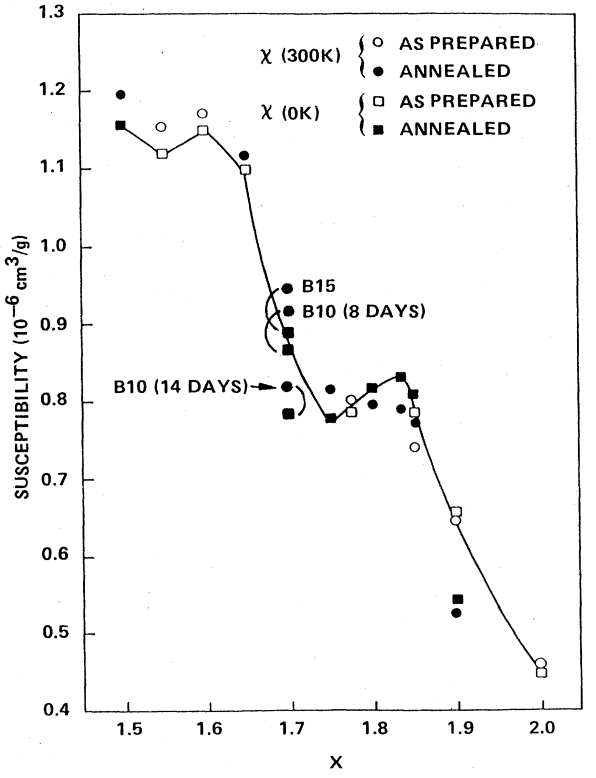

FIG. 13. Composition dependences of the 300 K magnetic susceptibilities $\chi(300\ \text{K})$ and the extrapolated parameter $\chi(0)$. The line drawn through the $\chi(0)$ data is a visual aid for the discussion in the text.

a negative temperature dependence [i.e., $\chi(0)$ exceeds $\chi(300\ \mathrm{K})$] only when $1.77 < x \leq 1.85$ just as seen in the proton σ_K and $(T_1T)^{-1/2}$ parameters.[6] Since the first derivative term in Eq. (4) will vanish near a $N(E)$ peak, the negative $\chi(T)$ temperature dependence again implies $d^2N(E)/dE^2 < 0$ at the Fermi level for $x \cong 1.83$. Hence, both the stoichiometry and temperature dependences of $\chi(T)$ are consistent with the $N(F_F)$ maximum for $ZrH_{1.83}$ proposed by BVCAS.

To the extent that comparisons are possible, the 525 °C anneals have modest influence on the $\chi(T)$ behavior as illustrated for $ZrH_{1.85}$ in Fig. 11. However, a large decrease in $\chi(T)$ is observed for $ZrH_{1.90}$ upon annealing as shown in Fig. 11. Virtually no differences in the lattice parameters or proton $(T_1T)^{-1/2}$ were noted for these samples. Hence, the $\chi(T)$ decrease is not likely to be caused by changes in $N(E_F)$ or the unit-cell properties. Furthermore, since emission-spectroscopy measurements performed on both samples after the $\chi(T)$ studies reveal essentially identical Fe contents (i.e., about 80 ppm), magnetic impurities do not appear responsible. The present XRD studies on annealed ZrH_x have suggested that oxygen solubility occurs to some extent at 525 °C. It may be that χ_{orb} term is reduced by the formation of a ternary $ZrO_yH_{1.90}$ phase. Further work will be necessary to clarify this behavior.

Some interesting observations are possible for the $\chi(T)$ values of the three annealed $ZrH_{1.70}$ samples shown in Fig. 12. From Fig. 13 it is clear that $\chi(T)$ for sample B15 (approximately equal contents of δ and ϵ phases) is almost exactly given by the average of the $\chi(T)$ values for δ-$ZrH_{1.65}$ and ϵ-$ZrH_{1.75}$, which is expected for a macroscopic property of a physical mixture. $\chi(T)$ for B10 (8-d anneal) is only slightly smaller where the relative amount of the ϵ phase is now somewhat greater as estimated from the intensities of the XRD patterns for the two phases. However, $\chi(T)$ for B10 (14-d anneal), which is pure ϵ phase, is much lower. Since the proton $(T_1T)^{-1/2}$ parameter for this sample is larger than for B15 (see Fig. 10), $N(E_F)$ is probably larger for B10 (14-d anneal). Consequently, its smaller $\chi(T)$ values are most likely due to the greatly reduced χ_{orb} contribution in the ϵ phase which masks any increase in the Pauli term to the susceptibility.

IV. CONCLUSIONS

Comparisons of the proton T_1 relaxation times, magnetic susceptibilities, and lattice parameters for as-prepared and annealed high-purity ZrH_x have shown that the tetragonal distortions induced as a Jahn-Teller effect[6] and the local peak in the density of states near the Fermi level are not altered by extended 525 °C anneals. The description of BVCAS for the ZrH_x electronic structure properties remains valid in general agreement with more recent band-theory calculations.[2] However, small systematic volume decreases upon annealing as well as changes the $ZrH_{1.70}$ (B10 sample) phase composition and the $\chi(T)$ parameters for $ZrH_{1.70}$ and $ZrH_{1.90}$ are tentatively attributed to the solution of "small" quantities of oxygen into the bulk. The discrepancies of the present results (as well as previous BVCAS and CBS studies) with some of the observations of Korn[7] are now believed to reflect the suspected larger concentrations of oxygen and paramagnetic impurities in Korn's samples. These impurities can strongly influence the phase compositions and physical properties of ZrH_x.

ACKNOWLEDGMENTS

We wish to thank Dr. A. Attalla for assistance with the sample handling; Dr. E. Jendrek and Dr. D. Sullenger for the computer programs used to analyze the XRD data; and E. Anderson, L. Brehm, and R. Ryan for the elemental analyses. This work was partially supported by the Chemical Sciences Division, Office of Energy Research, U. S. Department of Energy and the U. S. Department of Energy—Mound Research Participation Program. The Mound Facility is operated by Monsanto Research Corporation for the U. S. Department of Energy under Contract No. DE-AC04-76DP00053. Sandia National Laboratories are supported by the U. S. Department of Energy under Contract No. DE-AC04-76DP00789.

*Present address: Chemistry and Physics Laboratory, The Aerospace Corporation, Los Angeles, CA 90009.

[1]General reviews are (a) A. C. Switendick, in *Hydrogen in Metals I: Basic Properties*, edited by G. Alefeld and J. Völkl (Springer, Berlin, 1978), p. 101; and (b) A. C. Switendick, Z. Phys. Chem. Neue. Folge **117**, 89 (1979).

[2]A. C. Switendick, J. Less-Common Met. **101**, 191 (1984); A. C. Switendick, J. Less-Common Met. **103**, 309 (1984).

[3]F. Ducastelle, R. Candron, and P. Costa, J. Phys. (Paris) **31**, 57 (1970).

[4]J. H. Weaver, D. J. Peterman, D. T. Peterson, and A. Franciosi, Phys. Rev. B **23**, 1692 (1981).

[5]R. Göring, R. Lukas, and K. Bohmhammel, J. Phys. C **14**, 5675 (1981).

[6]R. C. Bowman, Jr., E. L. Venturini, B. D. Craft, A. Attalla, and D. B. Sullenger, Phys. Rev. B **27**, 1474 (1983).

[7]C. Korn, Phys. Rev. B **28**, 95 (1983).

[8]J. S. Cantrell, R. C. Bowman, Jr., and D. B. Sullenger, J. Phys. Chem. **88**, 918 (1984).

[9]V. Ya. Markin and V. N. Savin, Izv. Akad. Nauk SSSR—Neorg. Mater. **19**, 899 (1983) [Inorg. Mater. (USSR) **19**, 809 (1983)].

[10]H. A. Jahn and E. Teller, Proc. R. Soc. London, Ser. A **161**, 220 (1937).

[11]A. Narath, in *Hyperfine Interactions*, edited by A. J. Freeman and R. B. Frankel (Academic, New York, 1967), p. 287.

[12]M. Gupta and J. P. Burger, Phys. Rev. B **24**, 7099 (1981).

[13]Obtained from Materials Research Corporation, Orangeberg, NY 10962.

[14]R. C. Bowman, Jr., E. L. Venturini, and W.-K. Rhim, Phys. Rev. B **26**, 2652 (1982).

[15]T.-T. Phua, B. J. Beaudry, D. T. Peterson, D. R. Torgeson, R. G. Barnes, M. Belhoul, G. A. Styles, and E. F. W. Seymour, Phys. Rev. B **28**, 6227 (1983); T.-T. Phua, D. R. Torgeson, R.

G. Barnes, R. J. Schoenberger, D. T. Peterson, M. Belhoul, G. A. Styles, and E. F. W. Seymour, J. Less-Common Met. **104**, 105 (1984); and D. R. Torgeson, L.-T. Lu, T.-T. Phua, R. G. Barnes, D. T. Peterson, and E. F. W. Seymour, *ibid.* **104**, 79 (1984).

[16]W. L. Korst, U. S. Atomic Energy Commission No. NAA-SR-6880 (unpublished).

[17]K. G. Barraclough and C. J. Beevers, J. Nucl. Mater. **34**, 125 (1970).

[18]R. L. Beck and W. M. Mueller, in *Metal Hydrides,* edited by W. M. Mueller, J. P. Blackledge, and G. G. Libowitz (Academic, New York, 1968), p. 241.

[19]B. W. Veal, D. J. Lam, and D. G. Westlake, Phys. Rev. B **19**, 2856 (1979).

[20]N. N. Berezina, D. P. Valyukhov, and E. S. Vorontsov, Zh. Fiz. Khim. **55**, 2904 (1981) [Russ. J. Phys. Chem. **55**, 1650 (1981)].

[21]B. Holmberg and T. Dagerhamn, Acta Chem. Scand. **15**, 919 (1961).

[22]M. V. Nevitt, J. W. Downey, and R. A. Morris, Trans. Metall. Soc. AIME **218**, 1019 (1960).

[23]F. J. Rotella, H. E. Flotow, D. M. Gruen, and J. D. Jorgeson, J. Chem. Phys. **79**, 4522 (1983).

[24]A. J. Maeland, J. Less-Common Met. **89**, 173 (1983).

[25]The maximum value for y could be quite small (i.e., $y < 0.1$) due to electronic structure and/or volumetric effects. The precipitation of binary zirconium oxides is favorable under many conditions.

[26]P. Klavins, R. N. Shelton, R. G. Barnes, and B. J. Beaudry, Phys. Rev. B **29**, 5349 (1984).

[27]C. E. Ells and A. D. McQuillan, J. Inst. Met. **85**, 95 (1956).

[28]R. M. Cotts, in *Hydrogen in Metals I: Basic Properties,* edited by G. Alefeld and J. Völkl (Springer, Berlin, 1978), p. 227.

[29]C. Korn, Phys. Rev. B **17**, 1707 (1978).

[30]W. E. Wallace, in *Hydrogen in Metals I: Basic Properties,* edited by G. Alefeld and J. Völkl (Springer, Berlin, 1978), p. 169.

[31]R. C. Bowman, Jr., J. F. Lynch, and J. R. Johnson, Mater. Lett. 1, 122 (1982).

[32]R. C. Bowman, Jr., B. D. Craft, W. E. Tadlock, E. L. Venturini, and J. S. Cantrell, J. Appl. Phys. (to be published).

[33]U. Mizutani, N. Akutsu, and T. Mizoguchi, J. Phys. F **13**, 2127 (1983).

[34]R. A. Andrievskii, E. B. Baiko, and R. B. Ioffe, Izv. Akad. Nauk SSSR—Neorg. Mater. **3**, 1591 (1967) [Inorg. Mater. (USSR) **3**, 1385 (1967)].

[35]V. F. Nemchenko and V. G. Charnetskii, Izv. Akad. Nauk SSSR—Neorg. Mater. **10**, 456 (1974) [Inorg. Mater. (USSR) **10**, 392 (1974)].

[36]A. M. Clogston, B. T. Matthias, M. Peter, H. J. Williams, E. Corenzwit, and R. C. Sherwood, Phys. Rev. **125**, 541 (1962); J. A. Cape and R. R. Hake, *ibid.* **139**, A142 (1965).

[37]E. L. Venturini (unpublished).

[38]The contribution for parameter C_x becomes significant for temperatures below about 50 K.